

A&A manuscript no.
(will be inserted by hand later)

Your thesaurus codes are:
12(02.01.1; 02.14.1; 09.03.2; 10.01.1)

ASTRONOMY
AND
ASTROPHYSICS

Superbubbles and the Galactic evolution of Li, Be and B

Etienne Parizot

Dublin Institute for Advanced Studies, 5 Merrion Square, Dublin 2, Ireland; e-mail: parizot@cp.dias.ie

Received date; accepted date

Abstract. From a recent re-analysis of the available data, Be and B Galactic evolution appears to show evidence for a two-slope behaviour with respect to O. The inferred Be/O abundance ratio in halo stars is constant at very low metallicity (primary behaviour) and increases proportionally to O/H at high metallicity (secondary behaviour). We show that this can be explained in the framework of one single model, the ‘superbubble model’, in which Li, Be and B are produced by spallation reactions induced by energetic particles accelerated out of a mixture of supernova (SN) ejecta and ambient interstellar medium inside superbubbles (SBs). All the qualitative and quantitative constraints, including the energetics, the value of the transition metallicity and the ${}^6\text{Li}/{}^9\text{Be}$ isotopic ratio, are satisfied provided that the energetic particles have a spectrum flattened at low energy (in E^{-1}) and that the proportion of the SN ejecta inside SBs is of the order of a few percent. This lends support to Bykov’s acceleration mechanism inside SBs and to the SB dynamical evolution model of Mac Low & McCray (1988).

Key words: Acceleration of particles; Nuclear reactions, nucleosynthesis, abundances; ISM: cosmic rays; Galaxy: abundances

1. Introduction

The issue of Galactic chemical evolution is one of the most fundamental in astrophysics. How does one pass from the state of the universe following primordial nucleosynthesis, where virtually all the baryonic matter is composed of H and He nuclei (plus about ten percent of the current amount of ${}^7\text{Li}$), to a state in which the heavier chemical elements (i.e. the ‘metals’) exist in a sufficient proportion to form planets, rocks, crystals, plants, animals and the bodies of human beings? Most of these elements are synthesized in stellar cores or during the explosion of massive stars, and are released progressively in the interstellar medium (ISM), increasing the Galactic content in metals, i.e. the *metallicity*, Z . The case of Li, Be and B (LiBeB), however, is different. These *light elements* are believed

to be produced through spallation reactions induced by the interaction of energetic particles (EPs) in the ISM. In these reactions, an heavier nucleus (most significantly C, N or O) is ‘broken into pieces’, or *spalled*, and transmuted into one of the lighter ${}^6\text{Li}$, ${}^7\text{Li}$, ${}^9\text{Be}$, ${}^{10}\text{B}$ or ${}^{11}\text{B}$ nuclei. Except for ${}^7\text{Li}$, spallative nucleosynthesis is thought to be the main (if not the only) light element production mechanism. The case of ${}^{11}\text{B}$ is also slightly more complicated, as neutrino-induced spallation in supernovae (the so-called ν -process) is sometimes invoked to increase the B/Be and ${}^{11}\text{B}/{}^{10}\text{B}$ ratios which one would expect should the light elements be produced by nucleospallation alone.

Because of the spallative origin of LiBeB, the Galactic evolution of light elements is also relevant to nuclear and high energy astrophysics, as it provides unique constraints about the history of EP interactions in our Galaxy. While constraints about the *current* EP content of the Galaxy (i.e. cosmic rays as well as possibly other components) can be derived from gamma-ray astronomy and the study of ISM heating and ionization, information about the *past* EP populations can only be derived from integrated observables, such as the abundance of LiBeB in stars of various metallicities. These abundances are the outcome of ongoing LiBeB production from the ‘birth of the Galaxy’ to the time when the observed stars formed. Therefore, one can regard low-metallicity stars as astrophysical fossils giving evidence for the efficiency of nucleosynthetic processes over time, or in other words for the pace at which the chemical evolution of the various elements took place.

Assuming that the composition observed today at the surface of the stars reflects that of the gas from which they formed, one can follow the increase of the Be and B content of the Galaxy, say, as a function of metallicity. The inferred chemical evolution is thus not expressed with respect to the usual physical time, but with respect to what we can call a *chemical time*, defined as the abundance of metals in the ISM. In the approximation of a homogeneous Galaxy (without infall of primordial gas), the chemical time is a mere redefinition and a monotonically increasing function of the physical time. If the Galaxy is not chemically homogeneous, which is both expected and observed at early stages, then the chemical time has to be

defined locally and can be a non monotonic function of ordinary time (e.g. if dilution of high metallicity gas by low metallicity gas occurs; see Parizot & Drury 1999b).

A further complication, however, arises from the fact that the ISM metallicity proves to be a rather ambiguous measure of the chemical time. This is because the abundances of various elements are not found to increase proportionally to one another, and in particular the (most often used) O and Fe clocks do not appear to mark the same unambiguous chemical time. Indeed, according to some recent measurements, the O/Fe abundance ratio is *not* constant in the Galaxy, even at low metallicity, but decreases as a function of O/H (Israelian, et al. 1998; Boesgaard, et al. 1999; Mishenina, et al. 2000). This conclusion, however, is still controversial and there is no general consensus about which of the available methods (OI IR triplet, OI forbidden line, or OH molecular line) should be used to derive the O abundance whenever they are conflicting (see however Israelian et al. 2000, for a reconciliation between the various methods). It might therefore seem safer, when studying Be and B evolution from stellar abundances, to use the Fe abundance as the chemical time of reference, since it is in principle easier to measure. However it is O, not Fe, which is involved in the spallation reactions producing LiBeB, hence in a way Fe is totally irrelevant to the problem. In the absence of a chemical clock both reliable and relevant to light element Galactic evolution, we shall use here O as the reference element, and discuss LiBeB Galactic evolution as a function of O/H, keeping in mind that the exact numerical values might be reconsidered (or confirmed!) in the future, when a consensus about the various observational methods is reached.

2. Phenomenology and observational constraints

Among light elements the ${}^7\text{Li}$ isotope is characterized by a significant production by primordial nucleosynthesis, which accounts for about 10% of the total Li content of the Galaxy. In comparison, the contribution of Galactic nucleosynthesis (whether spallative or from AGB stars or novae) is negligible in the early Galaxy, and the Li stellar abundances are found to be almost constant at stellar metallicities lower than about 1/20th solar (e.g. Spite & Spite 1982). This implies that the early Galactic chemical evolution of Li is not constrained by the data, apart from being required to preserve the observed Spite plateau. In principle, this does not apply to ${}^6\text{Li}$, which is not produced by primordial nucleosynthesis any significantly. However, ${}^6\text{Li}$ represents such a tiny fraction of the total Li present in a low-metallicity star that the measurement of its specific abundance is a considerable observational challenge, which has been taken up for only two halo stars up to now (Hobbs & Thorburn 1994, 1997; Smith et al. 1998; Cayrel et al. 1999). Both of these stars have a metallicity around $[\text{Fe}/\text{H}] = -2.3$, and show a ${}^6\text{Li}$ abundance compatible

with a ${}^6\text{Li}/{}^9\text{Be}$ ratio between 20 and 80, in contrast with the solar value of ~ 6 .

As far as Be and B (BeB) are concerned, the contribution of primordial nucleosynthesis is entirely negligible so that the abundances measured in any low-metallicity star provide direct evidence about Galactic nucleosynthesis itself. From the phenomenological point of view, two specific behaviours can be identified for Be and B Galactic evolution:

- a *primary* behaviour, in which the Be and B abundances increase proportionally to O/H, so that the Be/O and B/O abundance ratios are constant, and
- a *secondary* behaviour, in which the Be and B abundances increase proportionally to the *square* of the O abundance, so that the Be/O and B/O ratios are proportional to O/H.

The first case is expected if the Be and B production rate is proportional to the rate of O release in the ISM, i.e. more or less to the SN explosion rate, while the second case corresponds to the standard scenario of Galactic cosmic ray nucleosynthesis (GCRN). Indeed, according to GCRN, Be and B are produced by spallation reactions induced by the interaction of EPs accelerated out of the ISM (namely, the cosmic rays) with the ISM itself (Reeves et al. 1970; Meneguzzi et al. 1971). The energy source of these EPs is the kinetic energy of the SNe, so that the power available for spallation is proportional to the SN explosion rate. Now the effective production of Be and B through spallation reactions depends on the abundance of O among the EPs and the ISM (since O is the main progenitor of Be and B). The total production rate is thus proportional not only to the rate of O release in the ISM, as in the first case above, but also to the O abundance itself, i.e. our chemical clock, O/H. This results in the secondary behaviour first described by Vangioni-Flam et al. (1990).

It has to be noted that the GCRN would also lead to a primary behaviour, *if the EP composition were constant and O-rich*. Indeed, most of the Be and B production would then be due to interactions of energetic O nuclei with the ISM, and thus be independent of the ambient O abundance. The Be and B production rates would then be simply proportional to the SN explosion rate, i.e. to the rate of O release in the Galaxy. One can thus conclude that, phenomenologically, a primary process is expected when the O abundance among the EPs is independent of (and higher than) that in the ISM, and a secondary process is expected when the EP composition reflects that of the ISM.

Now let us suppose that both a primary and a secondary process for BeB production exist in the Galaxy. Then for obvious reasons, and whatever their respective weight in the global Galactic ecology, the primary process is bound to dominated at very low metallicity, while the secondary process must dominate in the high metal-

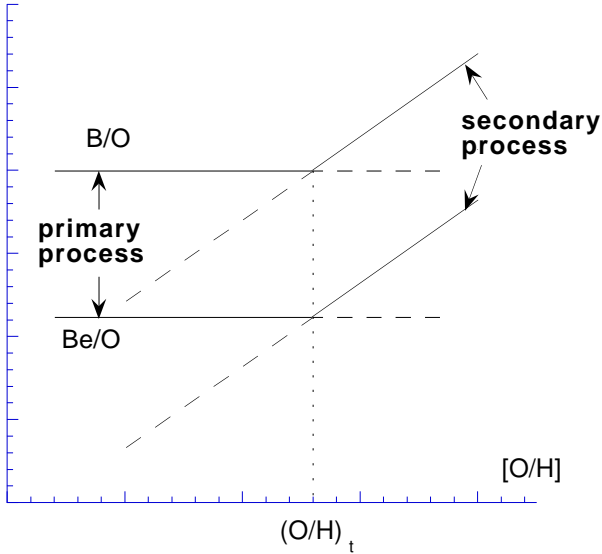


Fig. 1. Sketch of the expected Be and B evolution diagram in the case when both a primary and a secondary process exist in the Galaxy. The elemental ratios Be/O and B/O are shown as a function of O/H, in logarithmic scales.

licity limit. This is simply because the efficiency of the (idealized) secondary process is zero at $Z = 0$ and infinite at $Z \rightarrow \infty$. The abundance diagram showing Be/O and B/O as a function of O/H should then look like in Fig. 1, with a constant ratio below some *transition metallicity*, $Z_t \equiv (O/H)_t$, and a linearly increasing ratio above. Clearly, the precise determination of Z_t is an important goal for observational studies and would provide a strong constraint on the theoretical models of Galactic Be and B evolution.

In a recent study, Fields et al. (2000) have re-analyzed the available data about Be and B evolution as a function of O/H, discussing the uncertainties associated with the various methods used to derive the O abundance, the stellar parameters and the incompleteness of the samples. Their results are in conformity with the picture proposed above. In particular they have looked for evidence of a transition metallicity, using statistical analysis, and found a range of probable values of $\log(Z_t/Z_\odot)$ between -1.9 and -1.4 (see also Olive 2000). Above this metallicity, the Be and B evolution shows a secondary behaviour and seems compatible with the standard GCRN scenario. Unfortunately, very few data points have yet been reported below Z_t , and its exact value is rather uncertain. However, energetics arguments show that a primary process *is* indeed required below, say, $10^{-2}Z_\odot$ (e.g. Parizot & Drury 1999a,b; Ramaty et al., 2000a,b). This provides further support to the general ‘two-slopes’ scheme sketched out above, and in particular to the very existence of a transition metallicity (which is also certified up to a 99% confidence level by Fields et al., 2000). Since the energetics

argument has been somewhat controversial, we shall review in detail how it works in Sect. 3.

Beforehand, let us summarize the available observational evidence as follows:

1. the Be/O ratio observed in halo stars is constant up to a metallicity Z_t ,
2. below Z_t , $\text{Be/O} \sim 4 \cdot 10^{-9}$ (see Sect. 3),
3. Z_t is between $\sim 10^{-2}$ and $10^{-1.5}Z_\odot$,
4. above Z_t , $\text{Be/O} \propto \text{O/H}$,
5. at $Z = Z_\odot$, $\text{Be/O} \simeq 3.1 \cdot 10^{-8}$ (Anders & Grevesse 1989)

To these must be added the constraints relating to Li:

6. $\text{Li/Be} \lesssim 100$ for $Z \lesssim 10^{-1}Z_\odot$ (otherwise spallative nucleosynthesis breaks the Spite plateau),
7. ${}^6\text{Li}/{}^9\text{Be}$ is between 20 and 80 at $[\text{Fe/H}] \simeq -2.3$, i.e. $[\text{O/H}] \sim -1.5$ (with the observed O/Fe trend; Israelian et al., 2000), and
8. ${}^6\text{Li}/{}^9\text{Be} \simeq 6$ at solar birth.

Finally, the constraints relating to B read:

9. $10 \leq \text{B/Be} \leq 30$;
10. ${}^{11}\text{B}/{}^{10}\text{B} \simeq 4$ at solar birth;

In the following, we show that the so-called superbubble model for LiBeB production satisfies the whole of the above constraints with only one free parameter plus an additional mechanism for B production, e.g. the ν -process or nucleo-spallation induced by a component of low-energy cosmic rays (LECR). This model has been shown by Parizot & Drury (1999b) to offer a natural and efficient primary process for Be and B production in the very early Galaxy. Here, we argue that it also predicts the required change of behaviour (from primary to secondary) at a transition metallicity in the range derived by Fields et al. (2000) from the observational data (this prediction was actually implied by Fig. 3 of Parizot & Drury 1999b, and the related discussion, although not stated explicitly). In other words, the full range of ${}^6\text{LiBeB}$ evolution (i.e. below *and* above the primary-to-secondary transition) can be accounted for by one single mechanism, namely the acceleration of particles inside a superbubble (SB) out of a mixture of SN ejecta and ambient ISM.

In the following section, we review the GCRN energetics. The SB model is presented in Sect. 4, and the ingredients of the calculation are derived in Sect. 5. These ingredients are the composition and the energy spectrum of the superbubble energetic particles (SBEPs). In Sect. 6, we present the results relating to the evolution of the LiBeB abundances as a function of O/H. We discuss their implications in Sect. 7.

3. The energetics of GCRN

In this section, we intend to show that, whatever the assumption about the O/Fe trend in halo stars, the standard

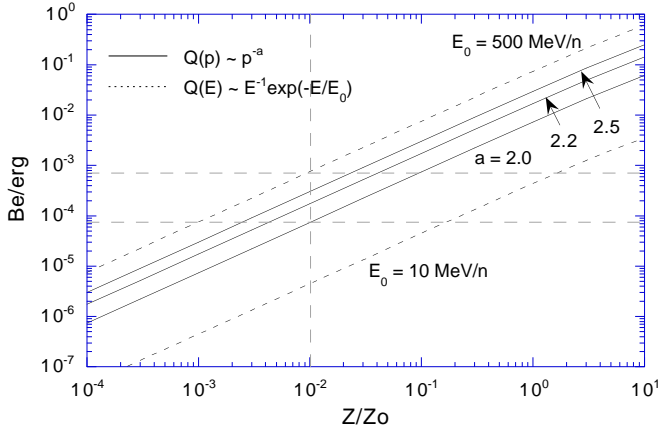


Fig. 2. Be production efficiency by spallation for different energy spectra, in numbers of Be nuclei produced per erg injected, as a function of the ISM (target) metallicity.

GCR nucleosynthesis cannot account for the Be abundance in low metallicity stars, because of energetics problems.

In their analysis, Fields et al. (2000) consider three sets of Be, B and O data (which they call the Balmer data, the IRFM1 data, and the IRFM2 data), differing by the choice of stellar parameters used to derive the abundances (see also Fields & Olive 1999). For the first two data sets, the resulting Be abundance found at $[O/H] = -2$ (i.e. $O/H = 10^{-2}(O/H)_\odot$) is consistent and equal to $Be/H = 2 \cdot 10^{-14}$. For the third data set, namely IRFM2, the Be abundance found at the same metallicity is somewhat higher: $Be/H \sim 3 \cdot 10^{-14}$ as derived from Fields' best model, and $Be/H \sim 5 \cdot 10^{-14}$ as derived directly from the data. In order to obtain a compelling conclusion, we use here the most conservative (i.e. lowest) value of $Be/H = 2 \cdot 10^{-14}$ at $[O/H] = -2$, i.e. $O/H = 5 \cdot 10^{-6}$ (Anders & Grevesse, 1989). The Be/O ratio is then $4 \cdot 10^{-9}$, which means that, on average, once integrated over the Galactic evolution up to the time when $[O/H]$ reaches -2 , the production of each nucleus of O must have been accompanied with the production of $4 \cdot 10^{-9}$ nuclei of Be. Considering that a SN produces on average $\sim 1.5 M_\odot$ of oxygen, i.e. $\sim 1.1 \cdot 10^{56}$ O nuclei, we end up with an average required production of Be of $\sim 4.5 \cdot 10^{47}$ nuclei per supernova (to be scaled linearly with the actual O yield one wishes to adopt for the SNe).

According to GCRN (and most models of Be production), the EPs responsible for the CNO spallation draw their energy from SN explosions. Therefore, assuming that about 10% of the SN energy is eventually imparted to the EPs, the total energy available for spallation is of order 10^{50} erg, which implies a Be production efficiency of $\sim 4.5 \cdot 10^{-3}$ nuclei synthesized per erg of EPs injected in the ISM. This efficiency has to be compared with the theoretical expectations. We have calculated the Be production efficiency as a function of the target metallicity for dif-

ferent EP energy spectra. The EP composition has been taken identical to the ISM composition, as appropriate for the GCRN scenario. The results are shown in Fig. 2. It should be noted that an increase of the metal abundances in the EPs of about a factor of 10, as could be invoked to conform to the current over-metallicity of the GCRs as compared to the mean ISM composition, does not change the results by more than a factor of 1.7 (upwards). As can be seen from Fig. 2, the Be production efficiency obtained for the GCRN, i.e. with the standard cosmic ray source spectrum in p^{-2} , is only $\sim 7.5 \cdot 10^{-5}$ Be/erg, namely a factor 60 below the required value (or even more if one considers that the value of $4.5 \cdot 10^{-3}$ derived above is actually the mean value of the Be production efficiency for $0 \leq Z_{\text{ISM}} \leq 10^{-2} Z_\odot$).

Allowing for a steeper slope of the cosmic ray source spectrum, namely $p^{-2.2}$ or even $p^{-2.5}$, does improve the situation, but not enough to reconcile the GCRN expectations with the observed amount of Be in low metallicity stars. Even with the most efficient spectrum, $Q(E) \propto E^{-1} \exp[-E/(500 \text{ MeV/n})]$ (see Sect. 5.2), the Be production efficiency obtained is still a factor 7 below the required value at $[O/H] = -2$, not mentioning the values at lower metallicity. We conclude that the standard GCRN cannot account for the production of Be and B in the early Galaxy, say for $Z \leq 10^{-2} Z_\odot$.

4. The superbubble model

As emphasized in Parizot & Drury (1999a,b), a simple solution to the above energetics problem consists in letting more metal-rich EPs interact with the ISM, so that the energetic carbon, nitrogen and oxygen nuclei (CNO) can be spalled in flight while propagating through the ISM and thereby increase the BeB production usually resulting mainly from energetic protons and α particles interacting with the ambient CNO. If the abundance of CNO among the EPs is large enough, these *reverse spallation* reactions can actually dominate the BeB production in the ISM and make the production efficiency independent of the ambient metallicity, in contrast with the situation shown in Fig. 2. This is typical of a primary production mechanism, which has been shown to be bound to dominate at very low metallicity. Since the CNO nuclei in the ISM originate from SN explosions, EPs with a high abundance of CNO can be obtained if particles are accelerated from a material contaminated by large amounts of SN ejecta. This is the case inside the superbubbles (SBs) which form consequently to the explosion of many SNe in an OB associations. Indeed, the dynamical effect of repeated SN explosions in a small region of the Galaxy is to blow large (super)bubbles of hot, rarefied material ($T > 10^6 \text{ K}$, $n \sim 10^{-2} \text{ g cm}^{-2}$), surrounded by shells of swept-up and compressed ISM. The interior of superbubbles consists of the ejecta and stellar winds of evolved massive stars *plus* a given amount of ambient ISM evapo-

rated off the shell and dense clumps passing through the bubble.

The exact composition of the particles to be accelerated inside the bubble depends on i) how much ambient material has evaporated towards the SB interior, ii) how well it is mixed with the SN ejecta, and iii) where the acceleration occurs, whether over the whole SB or more locally around the most recent SN explosion. If the material inside the superbubble is not well mixed, it is possible that the SBEPs be richer (or poorer) in CNO than the average material, depending on where exactly the acceleration takes place. None of the three questions above has yet received a conclusive answer, neither from theoretical nor observational studies. This explains why the superbubble models proposed so far to account for Be and B Galactic evolution (Parizot & Drury 1999b,2000; Ramaty, et al., 2000a,b; Bykov, et al., 2000) make different assumptions relative to the SB dynamics and to the acceleration process. In particular, the mass fraction of the SN ejecta inside the superbubble is of the order of a few percent if a thermal conduction model is used to evaluate the evaporation of the material from the supershell, while it would be much higher if the so-called ‘magnetic suppression’ mechanism occurred (Higdon et al. 1998). Likewise, the mixing of the ejecta with the ambient gas inside the bubble has been found to be efficient by Parizot & Drury (1999b), who compared the turbulent mixing time with the age of the SB, while Ramaty et al. implicitly assumed a relatively poor mixing. Finally, the acceleration mechanism has been assumed by Parizot & Drury to be of the Bykov type (Bykov & Fleishman 1992; Bykov 1995,1999), and thus more or less distributed over the whole SB, while Ramaty et al. use the standard shock acceleration model, and thus restrict the acceleration process to the vicinity of the latest SN explosion. Note that different EP energy spectra also result from these different assumptions (see below).

As indicated above, the current knowledge about superbubble dynamics does not allow one to decide between the models and to determine unequivocally the composition and spectrum of the SBEPs. From the point of view of nucleosynthesis, though, the SBEP composition and spectrum are the only ingredients we need to calculate the production rates of Li, Be and B and deduce their Galactic chemical evolution. Therefore, we propose here to proceed the other way round: first investigate the validity of the superbubble scheme for the LiBeB evolution, and second, use the available LiBeB data to constrain the SB models. To achieve the first point, we must show that the SB models naturally produce a Be evolution scheme in agreement with the available data, which applies to the qualitative *and* quantitative features. In other words, the SB models have to account for the total amount of Be found in the halo stars *and* the change of behaviour from a primary to a secondary evolution (with respect to oxygen) around a transition metallicity Z_t in the range currently allowed

by the data. Then we shall analyze more precisely the link between Z_t and the parameters of the SB so as to be able to draw sensible conclusions once Z_t is obtained with a greater precision from the data, hopefully in the near future. To this purpose, we now discuss the parameterization of the SB model and derive the relevant physical ingredients (for more details about the SB model itself, see Parizot & Drury 1999b,2000).

5. The physical ingredients of the model

5.1. The SBEP composition

Concerning the SBEP composition, we assume that the material accelerated inside the superbubble consists of a fraction x of pure SN ejecta, and a fraction $(1 - x)$ of the ambient material, i.e. gas with the ISM metallicity. As the general (or average) metallicity of the Galaxy increases, this ambient gas also gets richer and richer in heavy elements. Noting $\alpha_{ej}(X)$ and $\alpha_{ISM}(X)$ the abundances of element X among the SN ejecta and in the ISM, respectively, we can write the abundance of X among the SBEPs as:

$$\alpha_{SBEP}(X) = x\alpha_{ej}(X) + (1 - x)\alpha_{ISM}(X). \quad (1)$$

Physically, the single parameter x gathers all the information relative to the amount of evaporation off the SB shell and the dense clumps inside the SB (which governs the mass load of the SB by interstellar gas) and the effective mixing of the evaporated gas with the SN ejecta, before acceleration. The model obtained with $x = 1$ corresponds to the acceleration of pure ejecta, while $x = 0$ corresponds to the standard GCRN (acceleration of uncontaminated ISM).

In principle, the decomposition of the SBEPs into these two components (ejecta and ISM) can always be conceived in the abstract. Therefore the above parameterization does not introduce any simplification, as long as the acceleration mechanism is assumed to be non-selective (i.e. each chemical element is accelerated proportionally to its abundance). However, the value of the parameter x should be expected to vary from one SB to another, and to vary with time for each given SB, due to its dynamical evolution (Parizot & Drury, 1999b). As we show below, different values of x result in different SBEP composition and thus different LiBeB yields. The fact that x can be different for different SBs in the Galaxy therefore results in some scatter in the ${}^6\text{LiBeB}$ data. Additional causes for scatter in the data have been analyzed in detail in Parizot & Drury (2000) and we shall not consider these features here. Instead, we concentrate on the mean evolution of Be and B in the Galaxy and average our results over all the SBs participating to the ${}^6\text{LiBeB}$ enrichment. This amounts to using a single value of x in our models, thought of as the average of the individual x 's of individual SBs. In the same manner, we neglect the time-dependence of x resulting

Table 1. ISM abundances relevant to Be and B production, scaled with $Z_{\text{ISM}} \equiv \text{O}/\text{H}$ (f_{He} is given by Eq. 2).

Isotope	Abundance
^1H	$1.18 \cdot 10^3 / 10^{[\text{O}/\text{H}]}$
^4He	$1.18 \cdot 10^2 \times f_{\text{He}} / 10^{[\text{O}/\text{H}]}$
^{12}C	0.427
^{14}N	0.132
^{16}O	1.00

from the SB dynamical evolution (short time scale, $\sim 10^7$ yr). While the weight of the swept-up, evaporated ISM increases inside the bubble as time passes and more and more SNe explode, we use here an average x over the whole SB evolution. For results and discussion of the full time-dependent treatment, see Parizot & Drury (1999b). We also average over possible changes in the Galactic physical conditions, like for instance the mean ISM density and magnetic field (longer time scale, $\sim 10^8$ – 10^9 yr).

With the above parameterization, all we need to know to calculate the SBEP composition as a function of time (or mean ISM metallicity) is the composition of the ejecta and that of the ISM. The latter is assumed to be the solar composition (taken from Anders & Grevesse, 1989), with all the metals scaled in the same way. Concerning helium, we follow Ramaty et al. (1997) and adopt a slightly decreasing abundance with decreasing metallicity, to account for the He Galactic enrichment, from the primordial to the solar value. The function which we use is slightly different from that of Ramaty et al., and is given by:

$$f_{\text{He}}(Z_{\text{ISM}}) \equiv \frac{\alpha_{\text{ISM}}(\text{He})}{\alpha_{\odot}(\text{He})} = 1 + 0.0625 \log \left(\frac{Z_{\text{ISM}}}{Z_{\odot}} \right). \quad (2)$$

Note also that we scale the CNO abundances with O/H, rather than Fe/H. According to the recent O/Fe observations discussed in Sect. 1, the Fe abundance should not be scaled in the same way. However, this is not relevant to our calculations here because Fe does not significantly contribute to the LiBeB production. Table 1 summarizes our prescription for the ISM metallicity as a function of [O/H].

Finally, we need to specify the composition of the SN ejecta released in the interior of the superbubble. We use the models of Woosley & Weaver (1995). The exact composition depends on the mass of the SN progenitor and the explosion model used. However, since we wish to get information from the ensemble of the $^6\text{LiBeB}$ data, we use a mean composition obtained by averaging the yields of individual SNe over a Salpeter IMF (initial mass function). The results are shown in Table 2 for the relevant nuclei, as a function of the initial metallicity of the progenitor. It has to be noted that Woosley & Weaver (1995) used a Galactic chemical evolution model to generate abundances appropriate to every metallicity investigated. Although this model is not specified in the paper, it most

Table 2. SN yields (in M_{\odot}) of the elements relevant to Be and B production, as a function of the initial metallicity of the SN progenitor. The ejected masses of individual SNe have been taken from Woosley & Weaver (1995), models A, and averaged over a Salpeter IMF.

Z_{ISM}/Z_{\odot}	0.0001	0.01	0.1	1
^1H	9.0	8.8	8.8	8.0
^4He	6.6	6.7	6.8	6.8
^{12}C	0.19	0.20	0.20	0.21
^{14}N	1.5e-5	7.1e-4	6.6e-3	6.6e-2
^{16}O	1.1	1.4	1.5	1.5

probably does not take into account the O/Fe trend discussed above (which is incompatible with the SN explosion models, unless a non-standard chemical evolution model is used; see e.g. Ramaty, et al., 2000a,b). For this reason, the appropriate initial abundances should be different from those used in the explosion simulations. In the absence of any reliable prescription to modify the results accordingly, we use the published yields and assume that the quoted metallicity refers to the oxygen abundance (which is not really the case). Since the average yields appear to be almost independent of the initial metallicity for the nuclei of interest (H, He, C and O), the error introduced by being mistaken in the actual initial metallicities is expected to be negligible. Although the nitrogen yields are strongly dependent on the initial metallicity, the influence of this element on the total production of Be and B has been found marginal in any of our models.

From the SN yields of Table 2, we obtain the elemental abundances $\alpha_{\text{ej}}(\text{X})$ to be used in Eq. (1), and derive the abundances at intermediate metallicities by fitting the ‘data points’ linearly in logarithmic scale (power law). For completeness, we now give these fits for the number abundances of H, He, C and N, normalized to $\alpha_{\text{ej}}(^{16}\text{O}) = 1$. Writing the abundance of isotope X as $\alpha_{\text{ej}}(\text{X}) = A \times (Z_{\text{ISM}}/Z_{\odot})^B$, we obtain $(A, B) = (83.139, 0.048467)$ for ^1H , $(17.062, 0.034779)$ for ^4He , $(0.17435, 0.027322)$ for ^{12}C , and $(0.040795, 0.87048)$ for ^{14}N , from which we see that the abundances of H, He, C and O are almost constant in the SN ejecta, while the abundance of ^{14}N increases almost linearly with metallicity, as required for a secondary nucleus.

5.2. The SBEP energy spectrum

Concerning the SBEP energy spectrum, we investigate different shapes which we discuss below:

1. the standard cosmic ray source spectrum, $Q(p) \propto p^{-a}$, with $a = 2.0$, referred to as the ‘CRS2.0 spectrum’;
2. a modified (steeper) cosmic ray source spectrum, $Q(p) \propto p^{-a}$, with $a = 2.2$ or even $a = 2.5$, referred to as ‘CRS2.2’ or ‘CRS2.5’;

3. the so-called ‘weak SB spectra’, $Q(E) \propto E^{-1} \times \exp(-E/E_0)$, designed to mimic the results of Bykov’s acceleration mechanism in the case when most of the shocks responsible for particle acceleration inside the SB are weak shocks.
4. the so-called ‘strong SB spectrum’, matching the weak SB spectra below some break energy, E_{break} , $Q(E) \propto E^{-1}$ or equivalently $Q(p) \propto p^{-1}$, and the CRS2.0 spectrum above E_{break} , $Q(p) \propto p^{-2}$.

The first spectrum, ‘CRS2.0’, is motivated by the results of single shock acceleration models. We assume that it extends from 10 keV/n to 10^5 GeV/n. Although a higher cut-off is possible, our results only depend logarithmically on its actual value, through the amount of energy stored (and thus lost) in essentially unproductive high energy particles. The second spectrum, ‘CRS2.2’, is sometimes inferred for the cosmic-ray source spectrum by propagating backwards the observed GCR spectrum, assuming a plausible propagation model for the CRs in the ISM (e.g. Engelmann et al. 1990). As for the spectrum ‘CRS2.5’, it may be regarded as an *extreme* cosmic-ray source spectrum, and serves mainly as a ‘toy spectrum’ here, for investigation purposes.

The weak SB spectra have been used in previous works without clear physical justification. Their shape can be understood as follows. Considering that from the point of view of acceleration, the interior of a superbubble behaves as an ensemble of thousands of shocks with various velocities stochastically distributed over the SB volume (Bykov & Fleishman 1992), one can regard the SB acceleration model as a variant of multiple shock acceleration already investigated by several authors (see e.g. Marcowith & Kirk 1999, and references therein). In these models, the low-energy particles are accelerated very efficiently because their probability to escape from the shocks is very low: whenever a particle is advected away from one particular shock front, it can be ‘caught’ again by and flow through another shock in a different place. Remembering the general relation between the power-law index of particles accelerated at a single shock front and the escape and acceleration timescales: $f(p) \propto p^{-s}$, with $s = 3 + t_{\text{acc}}/t_{\text{esc}}$ (Kirk, et al. 1994), one sees that as the effective escape time tends to infinity in a multiple shock configuration, the power-law index of the EP distribution function tends towards 3. Now a distribution function $f(p) \propto p^{-3}$ is equivalent to an EP source spectrum in $Q(p) = f(p) \times 4\pi p^2 \propto p^{-1}$ in our notations, or $Q(E) = Q(p)(dp/dE) \propto E^{-1}$ in the non relativistic regime. This explains the shape of the weak SB spectra below the cut-off energy E_0 .

Clearly this spectral shape cannot hold up to the highest energies, since the total energy involved in EPs would then be strongly divergent above $E \sim m_p c^2$. In fact, a cut-off is expected in multiple shock acceleration models around an energy E_0 such that the diffusion length of the particles having this energy is comparable to the

inter-shock distance. For energies greater than E_0 , the assumptions normally used to derive the basic transport equation are violated, and the above arguments fail. A comparable change in the acceleration regime around this energy is also discussed by Bykov et al., and found to be responsible for the steepening of the particle distribution function. Following very crude arguments, one could expect the spectrum above E_0 to resemble the single-shock spectrum, $f(p) \propto p^{-s}$, where $s = 3r/(r-1)$ and r is the compression ratio across the shock discontinuity. Now most of the shocks are expected to be quite *weak* inside a superbubble (hence the name of the spectra), since they are mostly secondary shock, created by the reflection of a few primary shocks (from the SNe themselves or the stellar winds) over clumps of denser material or other strong or weak shocks. The compression ratios across these weak shocks are thus probably less than 2 and in fact possibly close to 1, which implies that the power-law index s is quite high. Interestingly enough, as long as s is greater than 4, which corresponds to the standard CRS2.0 spectrum and is obtained only for strong shock ($r = 4$), its exact value is not relevant to the calculations of LiBeB production because only a negligible amount of particles have energies above the energy E_0 around which the spectral shape changes. The bulk of the spallative LiBeB production inside the superbubble or in the surrounding shell is thus due to the interactions of SBEPs with energies below E_0 , so that the actual shape of the cut-off is unimportant. This is the reason why we adopt an exponential cut-off for the weak SB spectra instead of a power-law cut-off, in order to avoid an extra free parameter, and keep only E_0 as the relevant free parameter. According to Bykov & Fleishman (1992), E_0 is of the order of a few hundreds or a few thousands of MeV/n. We use here 500 MeV/n as a ‘canonical’ value for the cut-off energy, but we also explored other values and found no significant changes (except for $E_0 < 100$ MeV/n).

Finally, the ‘strong SB spectrum’ can be thought of as a SB spectrum in which the high energy particle distribution would match the standard cosmic-ray source spectrum. According to the above discussion, this would occur if most of the shocks accelerating the particles inside superbubbles were actually *strong* shocks (hence the name of the spectrum), with a compression ratio close to 4. In that case, the SBEPs could be but the GCRs observed at Earth. This ‘unifying scheme’ actually corresponds to the original ideas of Bykov & Fleishman (1992), and has already been proposed in the context of CR acceleration and LiBeB Galactic evolution (Higdon, et al. 1998; Ramaty & Lingenfelter 1999; Ramaty, et al., 2000a). In addition, it does not violate any available observation as the cosmic ray spectrum at low energy is not observable at Earth because of the solar modulation. We would then simply be able to predict a flattening of the GCR spectrum at low energy, approaching $Q(E) \propto E^{-1}$. Interestingly enough, we find that the ‘weak’ and ‘strong’ SB spectra give very

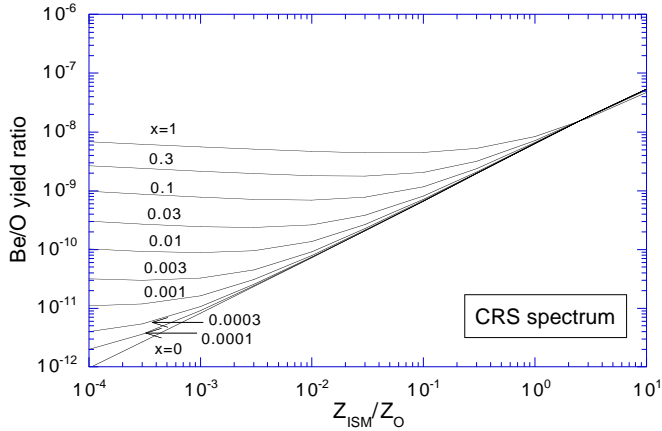


Fig. 3. Be/O yield ratio obtained with the CRS2.0 spectrum, as a function of the ambient metallicity, for various values of the mixing parameter, x . The Be yield is calculated for a total energy of 10^{50} erg imparted to the SBEPs.

similar results as far as the LiBeB production is concerned. For this reason, we may loosely refer below to any of the SB spectra as ‘the SB spectrum’. And since the LiBeB data do not constrain the SBEP spectrum at high energy (say above 1 GeV/n), both of the following views are possible: 1) the SBEPs have a spectrum extending up to energies of, say, 10^5 GeV/n, and are just the cosmic rays observed at Earth; or 2) the SBEP spectrum is cut at relatively low energy, so that the SBEPs cannot be the same EP component as the GCRs.

It is worth noting, however, that all the spectra described above have different implications for gamma-ray line astronomy as well as for the ionization and heating of the gas in the supershells and the adjacent molecular clouds. This means that additional constraints on the SBEP energy spectrum can be derived in principle from the calculation of the nuclear excitation rates and the ionization rate resulting from the interaction of the SBEPs with the ambient matter. These questions will be addressed elsewhere. In this paper, we focus on the implications of the different spectra for the LiBeB nucleosynthesis only, without any prejudice coming from other fields of astrophysics, to see whether the SB model can indeed account for the LiBeB observational data and what constraints can be derived from them. The ultimate goal, of course, will be to gather and combine all the possible constraints from various fields and improve our understanding of the acceleration mechanisms inside a superbubble and of the SBEP energy distribution.

6. The LiBeB production induced by the SBEPs

We now have all the ingredients necessary to calculate the Li, Be and B production induced by the interaction of the SBEPs with the ambient matter. While some of these interactions occur inside the superbubbles themselves, the

density there is so low that the corresponding LiBeB production is negligible as compared to that occurring in the dense regions surrounding the bubbles, namely the supershells and part of the molecular clouds from which the parent OB association formed. Dense clumps trapped inside the SBs can also provide efficient targets for the SBEPs. In all cases, the chemical composition of the target material is very close to the mean ISM composition at the time when the SBEP acceleration occurs. This allows us to close our problem, since we have already calculated the ISM composition as a function of Z_{ISM}/Z_{\odot} (see Table 1). Knowing the composition of the projectiles, their energy spectrum and the composition of the target, we can indeed calculate the various reaction rates by using the model described in Parizot & Lehoucq (1999). The relevant physical ingredients here are:

1. the spallation cross sections, taken from Read & Viola (1984) and various updates summarized in Ramaty et al. (1997);
2. the total inelastic cross sections from which we determine the probability for the projectiles to be destroyed before they give rise to a spallation reaction, and for the daughter nuclei (Li, Be or B) to be destroyed before they can thermalize and be ‘integrated’ to the ISM, so as to participate to the next episode of star formation (we use the semi-empirical values given by Silberberg & Tsao 1990);
3. the energy loss rates for the various nuclei in the medium of propagation, which compete with the nuclear reactions producing LiBeB. They have been kindly provided by Jürgen Kiener.

In order to compare the LiBeB production obtained from our SB models with the observational data, we first study the absolute Be production, as a function of the ISM metallicity, and then discuss the elemental and isotopic ratios of the three light elements.

6.1. Beryllium

To derive the Galactic evolution of beryllium, we compute the Be yield corresponding to the explosion of one supernova, and divide it by the yield of oxygen at the same metallicity, as interpolated logarithmically from Table 2. This allows us to obtain a Be/O yield ratio, which indicates how the Be content of the Galaxy evolves as a function of the metallicity, $[O/H]$. We have assumed that a total of 10^{50} erg per SN is imparted to the SBEPs, which amounts to approximately 10% of the SN kinetic energy. Such a value for the particle acceleration efficiency is quite typical of most acceleration models, but a simple scaling of our results is straightforward for more (or less) efficient acceleration mechanisms.

In Fig. 3, we show the Be/O yield ratio obtained for the CRS2.0 spectrum and various values of the dilution parameter, x , as a function of the ISM metallicity. It is

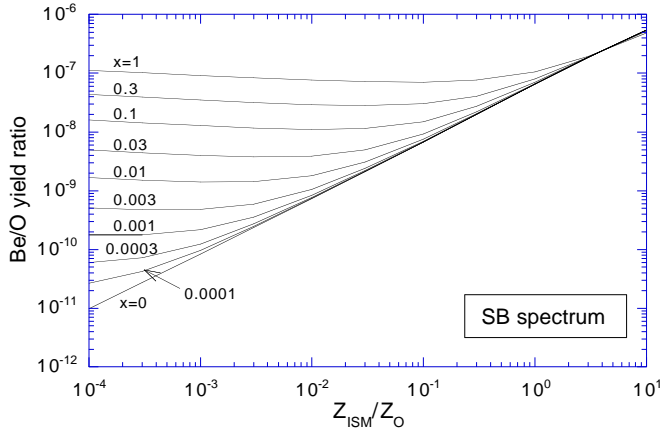


Fig. 4. Same as Fig. 3, but for the weak SB spectrum with a cut-off energy of 500 MeV/n.

obvious from these curves that each particular SB model, i.e. each particular value of x , leads to a Be evolution which is primary ($\text{Be}/\text{O} \sim \text{constant}$) below some transition metallicity, Z_t , and secondary ($\text{Be}/\text{O} \propto \text{O}$) above this metallicity, as required by the data. These qualitative features can be understood as follows. When the ambient metallicity is low, the metallicity of the SBEPs is dominated by the SN ejecta, except for very low values of the mixing parameter, x . This is easily seen from Eq. (1): when $Z_{\text{ISM}} = 10^{-4} Z_{\odot}$, say, the abundance of C, N and O is $\gtrsim 10^4$ times lower in the ISM than in the ejecta; therefore, most of the CNO present among the SBEPs come from the SN ejecta if $x \gtrsim 10^{-4}$. As a result, there is more CNO in the SBEPs than in the ISM and the Be production is dominated by reverse spallation reactions. For relatively large values of x , thus, the Be production efficiency is independent of the ambient metallicity, and the Be/O yield ratio is approximately constant (we even find slightly decreasing values because the relative weight of H and He in the SBEPs varies a bit and because the O yield itself is slightly increasing with Z_{ISM}). When the ISM metallicity increases, however, the fraction of the CNO present in the SBEPs coming from the ejecta decreases, because $\alpha_{\text{ISM}}(\text{CNO})$ in Eq. (1) scales with Z_{ISM} . The contribution of the fresh SN ejecta to the total Be yield then becomes marginal for sufficiently large values of Z_{ISM} , and the Be production efficiency is proportional to the ambient metallicity, as in the standard GCRN scenario. Indeed, the SB model is then equivalent to the GCRN since the SBEP composition is very close to that of the ISM. Unsurprisingly, thus, we find that the Be production efficiency and the Be/O yield ratio is proportional to Z_{ISM} for a sufficiently high ambient metallicity.

Most importantly, the transition metallicity at which the Be evolution changes from a primary behaviour ($\text{Be}/\text{O} \sim \text{constant}$) to a secondary behaviour ($\text{Be}/\text{O} \propto \text{O}$) depends on the mixing coefficient, x . This again is evident from Eq. (1). The more we put ejecta in the SBEPs (i.e.

the higher the parameter x), the later the secondary behaviour overcomes the primary one. Therefore, we can hope to predict the transition metallicity, Z_t , from a SB dynamical model (which would give the parameter x self-consistently) or alternatively we can constrain the SB evolution models from the value of Z_t derived from the observations. For example, Fig. 3 indicates that a transition metallicity between $[\text{O}/\text{H}] = -2$ and $[\text{O}/\text{H}] = -1.5$ implies that the SN ejecta represent between 1% and 10% of the SBEPs, which sets constraints on the SB evolution models and/or the mixing of the gas inside SBs (see Sect. 4 and below). However, the transition metallicity is not the only observable which one has to reproduce. As discussed in Sect. 3, the data obtained from halo stars imply that the Be/O yield ratio in the early Galaxy must be of order 4×10^{-9} . This is what we get from our model with the CRS2.0 spectrum, as shown in Fig. 3, if the mixing coefficient, x , is about 50%. But this is out of the range derived above. In other words, the two constraints (Z_t and Be/O) are in contradiction with one another if we assume for the SBEPs the CRS2.0 energy spectrum. We should also note that a value of x as high as ~ 0.5 is very hard to justify since it implies that the particles accelerated inside the superbubbles are almost pure ejecta, in contradiction with most SB evolution models which find a total mass inside the superbubble much larger than the mass of the ejecta (see e.g. Parizot & Drury 1999b, and below).

The situation is different, however, if one assumes that the particle acceleration does not occur over the whole volume of the superbubble, but only in those places where the ejecta of previous SNe have been released. But a theoretical justification and/or observational evidence for this is still lacking. Moreover, Fig. 3 shows that the transition metallicity corresponding to $x \sim 0.5$ is above $[\text{O}/\text{H}] \sim -1$, which also appears in contradiction with the data. Of course, if one allows for more than 10^{50} ergs to be imparted to the SBEPs per SN, all the curves on Fig. 3 can be shifted upwards and an agreement may be recovered between the range for x allowed by the Be/O constraint and that allowed by the preliminary results relating to Z_t . This, however, would not occur unless we increase the Be yield by a factor of ~ 20 , which amounts to put 2×10^{51} ergs into SBEPs, a rather unreasonable solution.

Much better appears to be the situation when the SB spectrum (either weak or strong) are used instead of the CRS2.0 spectrum. In Fig. 4, we show the results corresponding to the weak SB spectrum with the cut-off energy $E_0 = 500$ MeV/n. It can be seen that the correct Be/O yield ratio below $[\text{O}/\text{H}] = -2$ is obtained for a mixing coefficient of a few percent. This is particularly interesting since the ‘standard’ SB evolution models (in the smoothly distributed ISM) predict a very similar value for the fraction of the mass inside the bubble consisting of SN ejecta. Indeed, as discussed in Parizot & Drury (1999b), the SB mass derived from the non-magnetic evolution model (Weaver et al. 1977; Mac Low & McCray

1988) is given by:

$$M_{\text{SB}}(t) = (1600 M_{\odot}) L_{38}^{27/35} n_0^{-2/35} t_{\text{Myr}}^{41/35}, \quad (3)$$

where L_{38} is the mechanical luminosity of the OB association responsible for the growth of the superbubble, in units of $10^{38} \text{ erg s}^{-1}$, n_0 is the ambient density in cm^{-3} , and t_{Myr} is the time elapsed since the first SN explosion (in Myr). As a consequence, when 50 SNe have exploded, say, the time elapsed is about $t_{\text{Myr}} = 15.8$ (if $L_{38} = 1$) and the total mass of the gas inside the SB is $M_{\text{SB}} \sim 4.1 \cdot 10^4 M_{\odot}$. Considering that each supernova ejects, on average, $\sim 20 M_{\odot}$ of material, the total mass of the ejecta reaches about $1000 M_{\odot}$, i.e. $\sim 2.5\%$ of M_{SB} .

That this value is precisely in the range required to account for the Be/O ratio observed in halo stars is very remarkable, since we have not made any particular assumption to derive it. In other words, by using the standard SB evolution model and the standard efficiency for a particle acceleration model (i.e. $\sim 10\%$), one gets exactly the amount of Be production needed to explain the Be abundances observed in stars of metallicity lower than 10^{-2} solar. This should be considered as a strong argument in favour of both the SB model and the SB spectra. In addition, we see from Fig. 4 that the very same set of parameters also leads to a transition metallicity between $[\text{O}/\text{H}] = -2$ and $[\text{O}/\text{H}] = -1.5$, i.e. again exactly in the range suggested by the observational data. Both constraints are thus found to be consistent if one uses one of the SB spectra. And finally, it is possible to calculate the Be/O ratio predicted by this model at solar metallicity. To do so, we first need to recognize that the quantity plotted on the figures is not the stellar Be/O abundance ratio itself, but the Be/O yield ratio (i.e. ‘at production’). However, it is easy to derive one ratio from the other: focusing on the part of the curve above Z_t , we can write

$$\left. \frac{\text{Be}}{\text{O}} \right|_{\text{prod}}(t) = K \times \text{O}(t) \quad (4)$$

for the Be/O production ratio, where K is a constant which we do not need to specify here, and $\text{O}(t)$ is the total number of O nuclei in the ISM. Now the total number of Be nuclei in the ISM is given as a function of time by:

$$\begin{aligned} \text{Be}(t) &= \text{Be}(t_0) + \int_{t_0}^t \dot{\text{Be}}(t') dt' \\ &= \text{Be}(t_0) + \int_{t_0}^t \left. \frac{\text{Be}}{\text{O}} \right|_{\text{prod}}(t') \dot{\text{O}}(t') dt' \\ &= \text{Be}(t_0) + \int_{\text{O}(t_0)}^{\text{O}(t)} K \text{O} d\text{O} \\ &= \text{Be}(t_0) + \frac{K}{2} [\text{O}^2(t) - \text{O}^2(t_0)], \end{aligned} \quad (5)$$

where t_0 is the time corresponding to the transition towards the secondary behaviour of Be. Now acknowledging

that $\text{Be}(t_0)$ and $\text{O}(t_0)$ are negligible as compared to the solar values, we obtain $\text{Be}(t) \simeq \frac{1}{2} K \text{O}^2(t)$ from which we deduce the elemental abundance ratio at solar metallicity:

$$\left. \frac{\text{Be}(t)}{\text{O}(t)} \right|_{\odot} = \frac{1}{2} \times \left. \frac{\text{Be}}{\text{O}} \right|_{\text{prod}}(Z_{\odot}). \quad (6)$$

From Fig. 4 we see that the Be/O production ratio at solar metallicity is $\sim 6.6 \cdot 10^{-8}$. The ‘predicted’ value for the solar Be/O abundance ratio for this model is then $\sim 3.3 \cdot 10^{-8}$, remarkably close to the measured value, namely $3.1 \cdot 10^{-8}$ (Anders & Grevesse 1989)! We can thus report, in conclusion, that the SB model described above is fully consistent with the available data, and reproduces the whole scheme of Be evolution, both qualitatively and quantitatively, namely

1. the primary behaviour of Be up to Z_t ,
2. at the correct level of $\text{Be}/\text{O} \sim 4 \cdot 10^{-9}$,
3. the secondary behaviour above Z_t ,
4. with a value of Z_t consistent with the data,
5. and the correct value of the Be/O abundance ratio at solar metallicity.

Having shown that the SB model successfully describes the Galactic evolution of Be over the whole range of halo star metallicities, we now consider the case of the other light elements, Li and B, and see whether the LiBeB data can actually be used to set constraints on the SB dynamical evolution.

6.2. Lithium

The observational constraints on Li production by SBEP-induced spallation have been summarized in Sect. 2. In Fig. 5, we show the Li/Be yield ratios obtained with the CRS2.0 and the SB spectra, for different values of the mixing parameter, x . The general shape of the curves is easily understood if one realizes that Be is produced by CNO spallation only, while Li is produced by CNO spallation and $\alpha + \alpha$ reactions. As a consequence, higher Li/Be yield ratios are obtained for EP compositions richer in He. At a given metallicity, the latter correspond to lower values of x , i.e. smaller proportions of CNO-rich ejecta among the EPs. However, as the ambient metallicity increases, the weight of $\alpha + \alpha$ reactions decreases and the Li production becomes dominated by the CNO-spallation anyway, so that the spread in the Li/Be production ratios for different values of x decreases. As can be seen from the figures, the constraint $\text{Li}/\text{Be} < 100$ is respected for any SB model with a mixing parameter larger than $\sim 1\%$. This is in very good agreement with the range derived from the energetics constraint and the value of Z_t in the case of the SB spectrum.

Concerning ${}^6\text{Li}$, we found a ${}^7\text{Li}/{}^6\text{Li}$ isotopic production ratio in the range 1.3–1.7 for any value of x , any ambient metallicity and any SBEP spectrum. Such a ‘constancy’ of the isotopic production ratio is due to the fact that

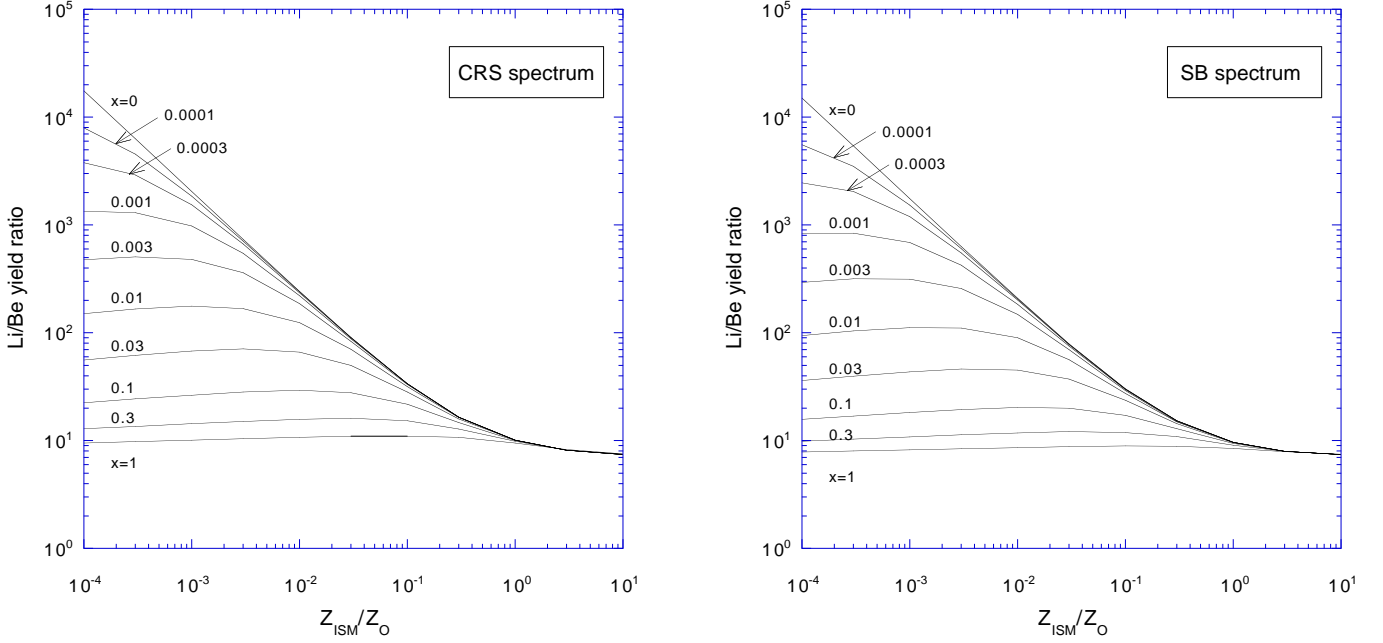


Fig. 5. Li/Be yield ratio of a superbubble as a function of the ambient metallicity, for various values of the mixing parameter, x . The SBEP spectrum is indicated on the figures.

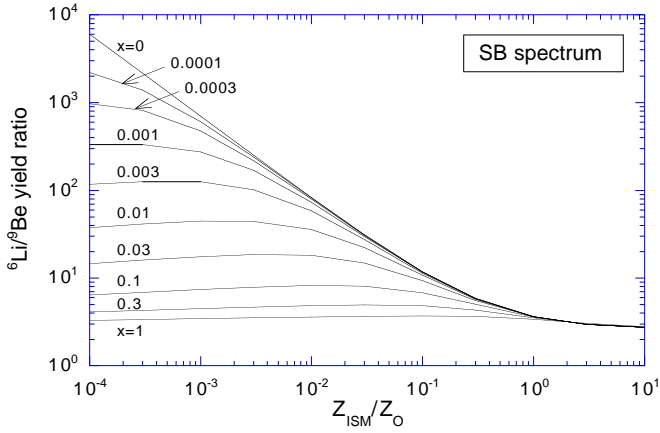


Fig. 6. ${}^6\text{Li}/{}^9\text{Be}$ yield ratio of a superbubble as a function of the ambient metallicity, for various values of the mixing parameter, x . The SBEP spectrum is the weak SB spectrum with a cut-off energy of 500 MeV/n.

${}^6\text{Li}$ and ${}^7\text{Li}$ are produced by the same nuclear reactions, with only slight variations in the reaction thresholds and resonances. The curves showing the ${}^6\text{Li}/{}^9\text{Be}$ production ratio as a function of metallicity can thus be roughly derived from Fig. 5, and we only show the exact results for the case of the SB spectrum with $E_0 = 500$ MeV/n, in Fig. 6. Interestingly enough, the ${}^6\text{Li}/{}^9\text{Be}$ production ratio at solar metallicity is virtually independent of the mixing parameter inside superbubbles, and is about ~ 3.6 . In order to compare this value with the solar value, ~ 6 , one has to average the ${}^6\text{Li}/{}^9\text{Be}$ production ratio over the whole Galactic evolution. Proceeding in the same spirit as

in Eq. (5), we have:

$$\left. \frac{{}^6\text{Li}}{{}^9\text{Be}} \right|_{\odot} = \frac{\int_0^{Z_{\odot}} \left. \frac{{}^6\text{Li}}{{}^9\text{Be}} \right|_{\text{prod}}(Z_{\text{ISM}}) \left. \frac{{}^9\text{Be}}{\text{O}} \right|_{\text{prod}}(Z_{\text{ISM}}) dZ_{\text{ISM}}}{\int_0^{Z_{\odot}} \left. \frac{{}^9\text{Be}}{\text{O}} \right|_{\text{prod}}(Z_{\text{ISM}}) dZ_{\text{ISM}}}. \quad (7)$$

Performing these integrations, we obtain $({}^6\text{Li}/{}^9\text{Be})_{\odot} \sim 5$, in reasonable agreement with the observed value. However, as we noted above, this constraint cannot be used to distinguish between the SB models, since different values of x and different EP spectra give roughly similar results, namely $({}^6\text{Li}/{}^9\text{Be})_{\odot}$ ratios between 3.5 and 5. On the other hand, Fig. 6 shows that the value of the ${}^6\text{Li}/{}^9\text{Be}$ ratio at lower metallicity is a very important observable, as it allows one to constrain the effective mixing parameter, x , very efficiently. Very remarkably, the first few data available at $\text{Fe}/\text{H} \simeq -2.3$ give ${}^6\text{Li}/{}^9\text{Be}$ between 20 and 80, which corresponds to a value of x in a range around one percent, in very good agreement with the values derived from the energetics and Z_t constraints. And once again, this agreement is achieved very naturally with the SB spectrum, while the higher value of x required for the CRS2.0 spectrum (see above) would imply a value of the ${}^6\text{Li}/{}^9\text{Be}$ ratio at low Z in contradiction with the observation. In this respect, we confirm that the model proposed by Ramaty et al. (2000a) in which the EPs have a constant metallicity all over the Galactic chemical evolution (which corresponds to a high x in our parameterization) cannot account for the ${}^6\text{Li}/{}^9\text{Be}$ ratio observed in halo stars. More data are expected to make this argument even stronger in the near future (or invalidate it, if in contradiction with the current data).

In any case, it is worth stressing again that the measurement of the ${}^6\text{Li}/{}^9\text{Be}$ ratio in low metallicity stars is very important, as it allows one to constrain the SB models very efficiently, in a way completely independent of the energetics. And as it stands, it is a strong argument in favour our model that all the available constraints, although independent from one another, namely energetics, Z_t and ${}^6\text{Li}/{}^9\text{Be}$, are in excellent agreement. Moreover, they indicate that the proportion of the ejecta inside SBs, x , is of the order of a few percent, and that the SBEP spectrum is close to the idealized SB spectrum discussed in Sect. 5.2. Both results have strong theoretical support from unrelated fields, namely SB dynamical evolution and SB particle acceleration (see above).

6.3. Boron

Finally, we turn to the case of boron. For all the SBEP spectra and compositions we have studied (i.e. for any value of x), we found B/Be production ratios between 10 and 12, for all ambient metallicities. As in the case of the ${}^7\text{Li}/{}^6\text{Li}$ production ratio, this is due to the fact that Be and B are produced by the same nuclear reactions, namely CNO spallation. The same is also true for the ${}^{11}\text{B}/{}^{10}\text{B}$ isotopic ratio, which is found between 2.0 and 2.3 for any value of the parameters. Comparing these values with the observational constraints recalled in Sect. 2, we find again the well-known result that spallation processes underproduce B, and in particular the ${}^{11}\text{B}$ isotope, with respect to other light elements. As noted above, this should not be considered as a failure of the model since other processes are known for B production (ν -process and LECR spallation) and have not been included here. In fact, the present results might be considered as indications that these other processes *must* be efficient in the Galaxy. This issue will be addressed elsewhere.

7. Conclusions and discussion

The SB model described above has been shown to be fully consistent with the qualitative and quantitative constraints of LiBeB Galactic evolution. Notably: 1) it explains the inferred two-slope behaviour in the framework of one single model; 2) it provides the correct value of Be/O at low metallicity; 3) it predicts the correct value of the transition metallicity; 4) it does not break the Spite plateau; 5) it is consistent with the ${}^6\text{Li}/{}^9\text{Be}$ ratio at all metallicity. Most importantly, these successes rely on the value of only one free parameter, namely the proportion of the SN ejecta inside a SB. Our calculations allow one to derive the value which best reproduces the data, namely a few percent, from the constraints of LiBeB evolution alone, i.e. without any external prejudice. However, it is remarkable that this value is exactly in the range expected from standard SB dynamical evolution models (Mac Low & McCray 1988). Likewise, the SB model is found to be

successful only if the EPs accelerated inside a superbubble have an energy spectrum flattened at low energy (in E^{-1}). Now this is just what Bykov's SB acceleration model predicts.

Interestingly enough, the consistency of the SB model is such that one may be tempted to reverse the argument and consider that the results of LiBeB Galactic evolution lend support to the current ideas about SB dynamical evolution and particle acceleration. Silich et al. (1996) have studied in detail the effect of the evaporation of the clouds engulfed inside superbubbles on their dynamical evolution. They assume that the ambient ISM is composed of small diffuse clouds with typical internal density of 10 cm^{-3} , and consider both cloud evaporation and dynamical disruption through internal flows inside the bubble. In the present context, these mechanisms would imply a modification of the mass loading of the superbubble and thus affect the expected proportion of the ejecta among the SBEPs. Although our results indirectly confirm the relevance of superbubble simulations in a smoothly distributed ISM, with only large-scale density gradients, the models taking into account a cloudy ISM cannot be rejected. In particular, Bykov (1999) has shown that in time-dependent models most of the acceleration occurs at relatively early times, when the contribution of cloud disruption and evaporation to the superbubble mass loading is small, according to the calculations of Silich et al. (1996).

As far as the particle acceleration inside superbubbles is concerned, we find that only an energy spectrum showing the characteristic shape of multiple shock acceleration at low energy ($Q(E) \propto E^{-1}$) is compatible with all the data. On the other hand, any SB spectrum is found to give very similar results. This means that LiBeB evolution alone cannot be used to determine whether the SBEPs extend to high energy or not. Above the so-called break energy, their spectrum could either match the standard CRS spectrum or decrease more steeply around an energy of a few hundreds or thousands of MeV/n. In the latter case, the SBEPs will have to be regarded as a second component of EPs in the Galaxy, in addition to cosmic-rays. In the opposite case, however, the SBEPs could be nothing but the GCRs and the SB model could then be thought of as a mere correction of standard GCRN, taking into account the chemical inhomogeneity of the early Galaxy. Indeed, GCRN assumes that the LiBeB-producing energetic particles are accelerated out of the average ISM. In a more detailed analysis, however, one has to acknowledge that the metals are released in localized regions of the Galaxy and abandon the homogeneous, one-zone representation. For it turns out that particle acceleration occurs precisely where the metals are more abundant. This is the essence of the SB model. It makes a crucial difference in the early Galaxy, when the chemical inhomogeneities are sharper (typically for $Z < Z_t$). But the value of the parameter x which we derived (a few percent) is small enough for

the chemical composition to be roughly identical inside and outside superbubbles today. This shows that the SB model and the GCRN model are essentially the same at metallicities $Z > Z_t$, i.e. for most of the lifetime of the Galaxy.

If the bottom line of the SB model is to account for chemical inhomogeneities, then it could actually apply to a wider context than SBs themselves. Localized star bursts would behave in about the same way, and globular clusters might also be considered as large OB associations giving rise to the same kind of phenomena, and thus participating to the LiBeB evolution in about the same way. The framework of LiBeB evolution described here would thus be quite general and only slight variations of the relevant parameters would occur from one environment to another, or from one place to another. These variations would cause possibly strong variation of the light elements-to-metals ratios from star to star, but all fitting in the same general pattern, namely a primary behaviour of ${}^6\text{LiBeB}$ up to a transition metallicity, Z_t , around 10^{-2} to $10^{-1} Z_\odot$, and a secondary behaviour afterwards. The resulting scatter in the LiBeB data has been discussed in Parizot & Drury (2000) (see also Cunha et al., 2000). In the spirit of the present paper, the scatter in the Be and B data can be evaluated by letting x vary from one SB to another, or as a function of time. This amounts to allow for some ‘diffusion’ across the curves represented in Figs. 3, 4 and 6. As an example, a variation of x by a factor of 3 (from 1% to 3%, say) would result in a variation of Be/O by the same factor at very low Z , while only by a factor of 2 at $[\text{O}/\text{H}] = -2$, and no variation at $Z = Z_\odot$.

Hopefully, improvements of the theoretical modeling of stellar atmospheres and the line formation will allow one to shorten the errors bars and measure the scatter in the data as a function of metallicity. Stronger constraints will thus be set on the LiBeB evolution models. Likewise, an accurate determination of the mass fraction of ejecta inside the SB can only be achieved if the transition metallicity, Z_t , is measured with enough precision. This requires data points at metallicities much lower than $[\text{O}/\text{H}] = -2$. As for the determination of the SBEP energy spectrum at high energy, it shall be more efficiently constrained by gamma-ray astronomy. An important challenge for the satellite INTEGRAL, to be launched in 2002, will be to detect nuclear de-excitation lines from EP interactions in nearby superbubbles (e.g. Orion or Vela). The expected gamma-ray fluxes have been estimated to be comparable with the INTEGRAL thresholds (Parizot & Knödseder, 1999a,b).

Finally, we wish to stress one of the important differences between the SB model, which accounts for the ‘two-slope behaviour’ of Be and B evolution within a single model, and an alternative scenario in which the low-metallicity (primary) part of the correlation would be attributed to one mechanism, and the secondary part to another mechanism (e.g. GCRN). In our model, the tran-

sition between the slope 1 and slope 2 Be-O correlation is continuous. Any intermediate value is reached over a given range of stellar metallicity (depending on the value of x). In the other case, by contrast, one would have a sharp change of slope at the precise metallicity where the secondary process becomes dominant, with no intermediate values. Of course, expected physical fluctuations of the parameters would weaken this effect, and current observational error bars prevent us from distinguishing conclusively between the two pictures. But we argue that the observed ‘slope 1.5’ behaviour reported by some authors (e.g. Boesgaard & Ryan, 2000) can be explained (in principle) only if there is a continuous *transition* from slope 1 to slope 2 within a *unique* model, rather than two unrelated models with a slope 2 eventually superseding a slope 1.

Acknowledgements. I wish to thank the International Astronomical Union and the organizers of the IAU 198 symposium on LiBeB evolution in Natal (Brazil), which stimulated this work. I was supported by the TMR programme of the European Union under contract FMRX-CT98-0168.

References

- Anders E., Grevesse N., 1989, *Geochim. Cosmochim. Acta* 53, 197
- Boesgaard A. M., Ryan S. G., 2000, in “The Light Elements and Their Evolution”, IAU Symposium 198, eds. L. da Silva, M. Spite, J. R. de Medeiros, in press
- Boesgaard A. M., King J. R., Deliyannis C. P., Vogt S. S., 1999, *AJ* 117, 492
- Bykov A. M., 1995, *Space Sci. Rev.* 74, 397
- Bykov A. M., 1999, in “LiBeB, cosmic rays and gamma-ray line astronomy”, ASP Conference Series, eds. R. Ramaty, E. Vangioni-Flam, M. Casse, K. Olive
- Bykov A. M., Fleishman G. D., 1992, *MNRAS* 255, 269
- Bykov A. M., Gustov M. Yu., Petrenko M. V., 2000, in “Astronomy with Radioactivities”, eds. R. Diehl, D. Hartmann, MPE Report 274, 241.
- Cayrel R., Spite M., Spite F., et al., 1999, *A&A* 343, 923
- Cunha K., Smith V. V., Parizot E., Lambert D. L., 2000, *ApJ*, in press
- Engelmann J. J., Ferrando P., Soutoul A., et al., 1990, *A&A* 233, 96
- Fields B. D., Olive K. A., 1999, *ApJ* 516, 797
- Fields B. D., Olive K. A., Vangioni-Flam E., Cassé M., 2000, submitted to *ApJ* (astro-ph/9911320)
- Higdon J. C., Lingenfelter R. E., Ramaty R., 1998, *ApJ* 509, L33
- Hobbs L. M., Thorburn J. A., 1994, *ApJ* 428, L25
- Hobbs L. M., Thorburn J. A., 1997, *ApJ* 491, 772
- Israelian G., García-López R. J., Rebolo R., 1998, *ApJ* 507, 805
- Israelian G., García-López R. J., Rebolo R., 2000, in “The Chemical Evolution of The Milky Way: Stars versus Clusters”, eds. F. Matteucci, F. Giovannelli, in press
- Kirk J. G., Melrose D. B., Priest E. R., 1994, *Plasma Astrophysics* Saas-Fee Advanced Course 24, Eds. A. O. Benz, T. J.-L. Courvoisier, Springer-Verlag, Berlin
- Mac Low M. M., McCray R., 1988, *ApJ* 324, 776

- Markowitz A., Kirk J. G., 1999, *A&A* 347, 391
- Meneguzzi M., Audouze J., Reeves H., 1971, *A&A* 15, 337
- Mishenina T. V., Korotin S. A., Klochkova V. G., Panchuk V. E., 2000, *A&A* 353, 978
- Olive K. A., 2000, in “The Light Elements and Their Evolution”, IAU Symposium 198, eds. L. da Silva, M. Spite, J. R. de Medeiros, in press
- Parizot E., Drury L., 1999a, *A&A* 346, 686
- Parizot E., Drury L., 1999b, *A&A* 349, 673
- Parizot E., Drury L., 2000, *A&A*, in press
- Parizot E., Knödlseeder J., 1999a, *Astrophysical Letters and Communications*, Vol. 38, 345
- Parizot E., Knödlseeder J., 1999b, to appear in *Proc. of the 19th Texas Symposium on Relativistic Astrophysics*, eds. J. Paul, T. Montmerle, E. Aubourg, in press
- Parizot, E., Lehoucq, R., 1999, *A&A* 346, 211.
- Ramaty R., Lingenfelter R. E., 1999, in “LiBeB, cosmic rays and gamma-ray line astronomy”, *ASP Conference Series*, eds. R. Ramaty, E. Vangioni-Flam, M. Casse, K. Olive
- Ramaty R., Kozlovsky B., Lingenfelter R. E., Reeves H., 1997, *ApJ* 488, 730
- Ramaty R., Scully S. T., Lingenfelter R. E., Kozlovsky B., 2000a, *ApJ*, in press (astro-ph/9909021)
- Ramaty R., Lingenfelter R. E., Kozlovsky B., 2000b, in “The Light Elements and Their Evolution”, IAU Symposium 198, eds. L. da Silva, M. Spite, J. R. de Medeiros, in press
- Read, S.M., Viola, V.E.Jr, 1984, *At. Data Nucl. Tables* 31, 359.
- Reeves H., Fowler W. A., Hoyle F., 1970, *Nature* 226, 727
- Silberberg R., Tsao C. H., 1990, *Physics Reports* 191, 351
- Silich S. A., Franco J., Palous J., Tenorio-Tagle G., 1996, *ApJ* 468, 722
- Smith V. V., Lambert D. L., Nissen P. E., 1998, *ApJ* 506, 405
- Spite F., Spite M., 1982, *A&A* 115, 357
- Vangioni-Flam, E., Cassé, M., Audouze, J., Oberto, Y., 1990, *ApJ* 364, 586.
- Weaver R., McCray R., Castor J., Shapiro P., Moore R., 1977, *ApJ* 218, 377
- Woosley S. E., Weaver T. A., 1995, *ApJSS* 101, 181